

PROGRESS AND TRENDS IN AIR INFILTRATION
AND VENTILATION RESEARCH

10th AIVC Conference, Dipoli, Finland
25-28 September, 1989

Paper 7

MULTIZONE FLOW ANALYSIS AND ZONE SELECTION USING A
NEW PULSED TRACER GAS TECHNIQUE

Patrick J. O'Neill and Roy R. Crawford

Department of Mechanical and Industrial Engineering
University of Illinois
Urbana, Illinois 61801
USA

NOMENCLATURE

A	= discrete-time system matrix
B	= discrete-time input matrix
c	= vector of tracer gas concentrations
D	= output matrix
F	= matrix of interzonal flows
G	= matrix used to represent $V^{-1}F$ during discrete to continuous inversion
g	= vector of applied inputs
I	= identity matrix
L	= least-squares gain matrix
M	= matrix whose columns are the eigenvectors of A
P	= matrix used during recursive least-squares algorithm
R	= matrix used to calculate V^{-1} formed from infinite series
v	= vector containing unmeasured system disturbances
V	= matrix containing effective volumes of zones
W	= transfer function matrix
y	= least-squares output vector
ϕ	= least-squares regression vector
θ	= least-squares parameter matrix
$\hat{\theta}(N)$	= least-squares estimate of θ based upon N observations
a_{ij}	= parameter appearing in input-output system formulation
b_{hq}	= parameter appearing in input-output system formulation
c'_i	= tracer concentration in zone i
\dot{c}'_i	= time derivative of tracer concentration in zone i
c_i	= (concentration of tracer in zone i) - (outdoor tracer concentration)
Δc	= concentration difference in two-zone system after impulse is applied
F_{ij}	= flow from zone i to j
F	= interzonal airflows of equal magnitude in a two zone system
g_i	= tracer input in zone i
h,i,j,k,q	= indices used for sequences or series
n	= total number of zones
N	= number of data points
p_{ij}	= parameter appearing in input-output system formulation
Q_i	= total flow into or out of zone i
$S(\theta)$	= total sum of the squared error using the indicated parameter matrix
s	= complex frequency variable defined in context of Laplace transform
T	= sampling interval
t	= time
T^*	= $T/(V/F_0)$; F_0 defined as total flow into a reduced order model
t^*	= $t/(V/F_0)$; F_0 defined as total flow into a reduced order model
V_i	= effective volume of zone i
$y_{i,act}$	= i th actual measured output
$y_{i,pred}^n$	= i th output predicted by an ARMA model of order n
z	= complex frequency variable defined in context of z transform
α	= constant used to set initial condition of P
β	= used during least-squares analysis to apply varying weights to the data
δ_{ij}	= Dirac delta function ($\delta_{ij} = 0$ for $i \neq j$; $\delta_{ij} = 1$ for $i=j$)
Δ	= constant used to bound maximum sampling interval
ε	= $\Delta c(t)/\Delta c(0)$
λ	= forgetting factor
μ	= eigenvalue of $V^{-1}F$
v_i	= eigenvector of A
σ^2	= variance
τ	= time constant for tracer decay
ω_i	= eigenvalue of A

1. SUMMARY

This paper presents and evaluates a new method, based upon tracer gas techniques, for determining interzonal airflows and effective volumes in a multizone enclosure. Presently used tracer gas techniques have a number of drawbacks including the need for multiple tracers when analyzing a multizone structure. Also, traditional techniques cannot be used to independently determine flows and volumes in the multizone case. The method described in this paper eliminates some of the problems introduced by multiple tracers and allows the independent determination of both flows and volumes.

The proposed method uses a single tracer gas to disturb the zones. A state-space formulation is used to model the multizone system. The concentration data are used in combination with a recursive least-squares identification algorithm to determine all of the interzonal airflows and effective volumes. A number of simulations are then used to validate the method. The simulations show that there are important considerations to keep in mind when selecting the type of input applied to each zone. They also indicate that the proper choice of sampling interval is critical for accurate identification.

The recursive least-squares formulation is readily adapted to the case where the system parameters are varying. A number of simulations show that this method can be used to track varying interzonal flows and effective volumes provided they are changing slowly with time.

Finally, a method for determining the number of interconnected zones in a system is introduced. The method uses a single impulse applied to one of the zones. The tracer concentration in that zone is then monitored. The data are fit to an autoregressive moving-average model and the residuals are analyzed using Akaike's AIC criterion which provides an indication of the order of the system.

2. INTRODUCTION

In recent years, increasing emphasis has been placed upon reducing overall building energy usage, while still maintaining acceptable levels of indoor air quality. As a tool in analyzing potential indoor air quality problem areas, tracer gas techniques have been employed with varying degrees of success (Harrje¹, Afonso², Jensen³, Axley⁴, Charlesworth⁵). Proper application of these techniques, whether based upon single or multiple tracers, can yield quantitative knowledge of the internal air circulation patterns.

If an accurate dynamic model of a building with respect to energy or mass transport is desired, the airflow measurement technique must determine the airflow rates, F , between zones and the effective volumes, V , of the zones as shown in Figure 1.

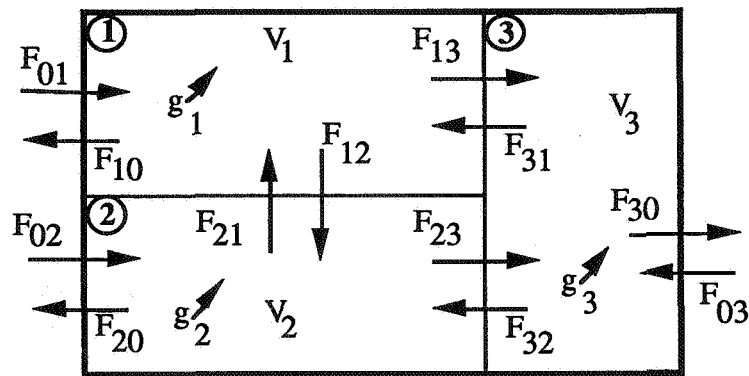


Figure 1. Three-Zone Airflow and Volume Model

The flows between zones can be the result of either mechanical (forced ventilation system) or natural convection (open doors or windows). Many buildings contain some combination of these two and most tracer gas techniques do not differentiate between them.

The effective volume is the volume of the interior of a zone in which complete mixing occurs (Allen⁶). In order to determine interzonal airflows, most tracer techniques assume that the effective volume is known a priori. For example, the effective volume might be assumed to be nearly equal to the unfilled volume of a room. However, if dead zones or ventilation system short circuiting occurs, the results of these techniques may be completely erroneous. Accurate determination of the effective volume will ensure not only robust control of indoor air quality and human comfort but will also indicate areas where improvements are needed.

This paper further evaluates a new method (O'Neill⁷), based upon tracer gas techniques, for determining interzonal airflows and effective volumes in a multizone enclosure. The method uses inputs of a single tracer gas to disturb each of the zones. A state-space formulation is used to model the multizone system and the concentration data were used in combination with a least-squares identification algorithm to determine all of the interzonal airflows and effective volumes.

Several issues which arise during the implementation of this and other tracer gas techniques are also addressed. These include:

- required length of test
- sampling period based upon:
 - numerical stability of identification algorithm
 - system dynamics
- input requirements
- identifying the number differentiable zones
- varying flows and/or effective volumes

3. MULTIZONE MODEL FORMULATION

For a multizone system as shown in Figure 1, conservation of mass for the tracer gas in a single zone, i , can be written as (Sinden⁸)

$$V_i(t) \dot{c}'_i(t) = \sum_{j=0}^n (1-\delta_{ij})F_{ji}(t)c'_j(t) - c'_i(t) \sum_{j=0}^n (1-\delta_{ij})F_{ij}(t) + g_i(t) \quad (3.1)$$

where

- $g_i(t)$ = tracer input into zone i (mass/time)
- $V_i(t)$ = effective volume of zone i
- $c'_i(t)$ = tracer concentration in zone i (mass/volume)
- $\dot{c}'_i(t)$ = time derivative of tracer concentration in zone i (mass/volume·time)
- $F_{ij}(t)$ = flow from zone i to j (volume/time)
- δ_{ij} = Dirac delta function ($\delta_{ij} = 0$ for $i \neq j$; $\delta_{ij} = 1$ for $i=j$)
- n = total number of zones

The subscript "0" represents outdoor air. For the remaining theoretical analysis and simulations to follow, units will be omitted from the numerical results. These numbers may either be considered dimensionless or have units consistent with those defined in Equation (3.1). Also, for the remainder of the analysis, the concentration of tracer in the outdoors will be considered constant or relatively slowly changing. If this approximation is made, the outdoor concentration, c'_0 , can be eliminated from Equation (3.1) by defining the other concentration terms to be the difference between the actual zone concentration and the outdoor value

$$c_i \equiv c'_i - c'_0 \quad (3.2)$$

Equation (3.1) represents n first-order simultaneous differential equations for the multizone system. For the case where $n = 3$, Equation (3.1) could be written in state-space form as

$$\begin{bmatrix} V_1(t) & 0 & 0 \\ 0 & V_2(t) & 0 \\ 0 & 0 & V_3(t) \end{bmatrix} \begin{bmatrix} \dot{C}_1(t) \\ \dot{C}_2(t) \\ \dot{C}_3(t) \end{bmatrix} = \begin{bmatrix} -Q_1(t) & F_{21}(t) & F_{31}(t) \\ F_{12}(t) & -Q_2(t) & F_{32}(t) \\ F_{13}(t) & F_{23}(t) & -Q_3(t) \end{bmatrix} \begin{bmatrix} C_1(t) \\ C_2(t) \\ C_3(t) \end{bmatrix} + \begin{bmatrix} g_1(t) \\ g_2(t) \\ g_3(t) \end{bmatrix} \quad (3.3a)$$

where

$$Q_i(t) = \sum_{j=0}^n (1-\delta_{ij})F_{ij}(t) = \sum_{j=0}^n (1-\delta_{ij})F_{ji}(t) \quad (3.3b)$$

In Equation (3.3) the term $Q_i(t)$ represents the total flow into or out of zone i.

Equation (3.3) can be represented more compactly in matrix form as

$$V(t) \dot{c}(t) = F(t) c(t) + g(t) \quad (3.4)$$

or multiplying through by $V^{-1}(t)$

$$\dot{c}(t) = V^{-1}(t)F(t) c(t) + V^{-1}(t)g(t) \quad (3.5)$$

Equation (3.5) is known as the time varying state-space representation of the system of linear differential equations described by Equation (3.1). At this point, it is not

necessary to assume that the matrices $V(t)$ and $F(t)$ are constant for the entire duration of the tracer gas test.

The least-squares algorithm described below requires that the system be represented in discrete form. If it is assumed that the flows, $F(t)$, volumes, $V(t)$, and input, $g(t)$, are held constant during the sampling interval, T , Equation (3.5) can be written as (Kuo⁹)

$$c[(k+1)T] = A c(kT) + B g(kT) \quad (3.6)$$

where A and B are defined as

$$A = \exp[(V^{-1}F)T] = I + (V^{-1}F)T + \frac{[(V^{-1}F)T]^2}{2!} + \frac{[(V^{-1}F)T]^3}{3!} + \dots \quad (3.7)$$

$$B = \int_0^T \exp[(V^{-1}F)t] V^{-1} dt = \left[IT + \frac{(V^{-1}F)T^2}{2!} + \frac{(V^{-1}F)^2 T^3}{3!} + \dots \right] V^{-1} \quad (3.8)$$

with V^{-1} and F defined as the values of $V^{-1}(t)$ and $F(t)$ on the interval $(kT, [k+1]T)$. Equation (3.6) is the linear discrete-time state-space formulation of the system described in Equation (3.1) with $k = t/T$.

4. RECURSIVE LEAST-SQUARES IDENTIFICATION ALGORITHM

The problem of parameter identification has been studied extensively in many fields as a necessary first step in any type of system analysis (Ljung¹⁰, Eykhoff¹¹, Kudva¹², Ossman¹³). One well known procedure used in parameter estimation is known as the method of least-squares. In this method, a model form containing one or more unknown parameters is assumed to describe the system. One or more tests are then run in which known inputs are applied and the outputs of the system are measured. These data are then used to select the best combination of parameters with respect to minimizing the sum of the squared error between the actual data and the predicted value.

To formulate the least-squares estimate of the system parameters, Equation (3.6) is rewritten in a slightly different form

$$y[k] = \theta^T \phi(k-1) + v(k-1) \quad (4.1)$$

where $y[k]$ is a vector containing the measured tracer concentrations in each zone at time step k . The symbol, θ , is used to denote the parameter matrix,

$$\theta = [A \ B]^T \quad (4.2)$$

and contains the unknown parameters of interest. The variable, $\phi(k-1)$, is the regression vector whose components are comprised of past observations of the inputs and outputs of the system (regression variables)

$$\phi(k-1) = [c_1(k-1) \ c_2(k-1) \dots c_n(k-1) \ g_1(k-1) \ g_2(k-1) \dots g_n(k-1)]^T \quad (4.3)$$

The vector, $v(k-1)$, contains unknown and unmeasurable disturbances to the system (eg. measurement noise).

The method of least-squares is described by the criterion function

$$S(\theta) = \sum_{k=1}^N \beta(k) \{ [y^T[k] - \phi^T(k-1)\theta] [y[k] - \theta^T\phi(k-1)] \} \quad (4.4a)$$

$$= \sum_{k=0}^{N-1} \beta(k) v^T(k) v(k) \quad (4.4b)$$

assuming $v(k)$ is a sequence of random variables with zero mean (white noise). In Equation (4.4), the term, N , is the number of data points collected and $\beta(k)$ is a sequence which can be used to give varying weights to different data. The optimal choice of the parameter vector is that vector which minimizes $S(\theta)$ —producing the smallest summation of the squared errors. Since Equation (4.4) is quadratic in θ , it is straightforward to solve analytically. This gives

$$\hat{\theta}(N) = \left[\sum_{k=1}^N \beta(k) \phi(k-1) \phi^T(k-1) \right]^{-1} \sum_{k=1}^N \beta(k) \phi(k-1) y^T(k-1) \quad (4.5)$$

$\hat{\theta}(N)$ is the least-squares estimate, based upon N observations, of the actual parameter matrix θ .

The method of determining the unknown system parameters by first collecting all of the data and then calculating $\hat{\theta}(N)$ using Equation (4.5) is known as the batch method. The batch method is useful for systems which are well understood and prior knowledge about when to apply the inputs is known. However, it is often more useful to represent Equation (4.5) in a recursive fashion. With a recursive identification algorithm, the unknown parameters can be calculated as each new data point is recorded.

While the derivation of the recursive form of Equation (4.5) is straightforward, it is somewhat algebraically involved (See Ljung¹⁰ or Eykhoff¹¹). Therefore, just the results will be presented here. The recursive least-squares algorithm is simple in concept. Using this procedure, the new estimate of the parameter matrix, $\hat{\theta}(k)$, is equal to the old estimate, $\hat{\theta}(k-1)$, plus some gain matrix, $L(k)$, times the error between the predicted and actual values of the output(s). The algorithm is thus,

$$\hat{\theta}(k) = \hat{\theta}(k-1) + L(k) [y^T[k] - \phi^T(k-1) \hat{\theta}(k-1)] \quad (4.6a)$$

where

$$L(k) = \frac{P(k-1) \phi(k-1)}{1/\beta(k-1) + \phi^T(k-1) P(k-1) \phi(k-1)} \quad (4.6b)$$

$$\mathbf{P}(k) = \mathbf{P}(k-1) - \frac{\mathbf{P}(k-1)\phi(k-1)\phi^T(k-1)\mathbf{P}(k-1)}{1/\beta(k-1) + \phi^T(k-1)\mathbf{P}(k-1)\phi(k-1)} \quad (4.6c)$$

Therefore, the most computationally involved part of the algorithm comes in computing the gain matrix, $\mathbf{L}(k)$.

Examination of Equation (4.6) leaves the question of initial conditions of the matrices $\hat{\theta}(k_0)$ and $\mathbf{P}(k_0)$ as yet unresolved. As $N \rightarrow \infty$ the effect of the initial values disappears. In practice however, even for a small number of data points, the effect of initial conditions is negligible. Thus, common choices for the initial values of $\mathbf{P}(k_0)$ and $\hat{\theta}(k_0)$ are $\mathbf{P}(k_0) = \alpha\mathbf{I}$ and $\hat{\theta}(k_0) = \mathbf{0}$, where α is some large constant. However, if an 'exact' initial guess is desired or only a few data points are available, the following values of $\mathbf{P}(k_0)$ and $\hat{\theta}(k_0)$ should be used

$$\mathbf{P}(k_0) = \left[\sum_{k=1}^{k_0} \beta(k)\phi(k-1)\phi^T(k-1) \right]^{-1} \quad (4.7a)$$

$$\hat{\theta}(k_0) = \mathbf{P}(k_0) \sum_{k=1}^{k_0} \beta(k)\phi(k-1)y(k-1) \quad (4.7b)$$

The value of k_0 in Equations (4.7a) and (4.7b) should be chosen such that the required matrix inversion is possible.

The recursive least-squares method allows one to examine, in real time, the response of the system parameters to the applied inputs and determine when (and possibly where) new inputs should be applied. For example, if one or more inputs have been applied in the past and the parameters of interest are no longer changing appreciably with each new data point collected, then it is appropriate to apply an additional input or terminate the test.

5. INVERSION FROM A AND B TO V AND F

Before evaluating the least-squares algorithm described above, some discussion is necessary on how to interpret the values of the flows, F , and effective volumes, V , from the matrices \mathbf{A} and \mathbf{B} . In the development of Equation (3.6), it was not necessary to approximate the differentials appearing in Equation (3.5). Thus, the values of \mathbf{A} and \mathbf{B} obtained during the least-squares analysis are not affected by any such approximations. However, when going in the opposite direction, that is, calculating F and V from \mathbf{A} and \mathbf{B} it is not as simple.

Depending upon the length of the sampling interval, different approaches may be necessary. If the sampling period is short, relative to the system eigenvalues, then an Euler approximation (forward differencing) may be adequate. For example, if the Euler approximation is made, the differential is written as

$$\dot{c}(t) = \frac{c([k+1]T) - c(kT)}{T} \quad (5.1)$$

and Equation (3.6) becomes

$$c[(k+1)] = (I+TV^{-1}F) c(k) + TV^{-1} g(k) \quad (5.2)$$

thus,

$$V = TB^{-1} \quad (5.3a)$$

$$F = V(A - I)/T \quad (5.3b)$$

Examination of Equations (3.7) and (3.8) show that the Euler approximation is equivalent to using the first two terms of the infinite series for A and the first term in the infinite series for B. Tustin's and other higher order approximations are obtained in a similar manner. In practice, it has been found that using the first several terms from each series is adequate in most cases.

When larger sampling intervals are used however, the higher order terms in the series remain significant. Here, the simple approximations described above may not prove adequate. One method for circumventing difficulties associated with larger sampling intervals uses properties of eigenvalues and eigenvectors in the calculation of the exponential of a matrix (Sinha¹⁴).

If the eigenvalues, $\omega_1, \omega_2, \dots, \omega_n$ are distinct the eigenvectors v_1, v_2, \dots, v_n of the matrix A can be calculated (In case of multiple eigenvalues, the eigenspace must have equal multiplicity) then it is possible to form the matrix M

$$M = [v_1 \ v_2 \ \dots \ v_n] \quad (5.4)$$

which will diagonalize A. The quantity $V^{-1}F$ is given by forming the following equality

$$V^{-1}F = G = \left\{ M \text{diag} \left[\frac{1}{T} \ln \omega_1 \quad \frac{1}{T} \ln \omega_2 \quad \dots \quad \frac{1}{T} \ln \omega_n \right] M^{-1} \right\} \quad (5.5)$$

If A has negative eigenvalues, the logarithms in Equation (5.5) become undefined. This problem is eliminated by proper selection of sampling interval and will be discussed in a following section. Finally, the matrix V is given by

$$V = B^{-1}R \quad (5.6)$$

where the matrix R is defined as

$$R = IT + \frac{GT^2}{2!} + \frac{G^2T^3}{3!} + \dots \quad (5.7)$$

6. SIMULATIONS USING THE LEAST-SQUARES ALGORITHM

The algorithm described by Equation (4.6) was tested on various multizone systems using computer generated data, $\beta(k)=1$. The interzonal flows and volumes were picked arbitrarily and chosen so that the system was asymmetric. The algorithm

was tested for systems with one, two, and three-zones. Table 1 shows the results of these simulations for the case of clean data (no noise) and also for cases of data with low and moderate measurement noise. The noise added to the simulation data were random variables with a maximum value equal to a fixed percentage of the zones initial concentration. The maximum values of the noise used in the simulations were 5 and 10% and resulted in variances of $\sigma^2 = 0.002$ and 0.008 .

Table 1. Identification of Flows and Effective Volumes using Least-Squares Algorithm

# of Zones	Noise σ^2	V ₁	V ₂	V ₃	F ₀₁	F ₁₀	F ₀₂	F ₂₀	F ₀₃	F ₃₀	F ₁₂	F ₁₃	F ₂₁	F ₂₃	F ₃₁	F ₃₂
1	0.00	1006	-	-	.20	.20	-	-	-	-	-	-	-	-	-	-
1	0.002	998	-	-	.21	.21	-	-	-	-	-	-	-	-	-	-
1	0.008	986	-	-	.21	.21	-	-	-	-	-	-	-	-	-	-
Actual	-	1000	-	-	.20	.20	-	-	-	-	-	-	-	-	-	-
2	0.00	1023	2031	-	.10	.29	.50	.31	-	-	.21	-	.41	-	-	-
2	0.002	1010	1970	-	.11	.27	.53	.28	-	-	.25	-	.43	-	-	-
2	0.008	964	2107	-	.09	.35	.55	.31	-	-	.23	-	.48	-	-	-
Actual	-	1000	2000	-	.10	.30	.50	.30	-	-	.20	-	.40	-	-	-
3	0.00	1006	2017	3021	.00	.10	.31	.00	.00	.21	.42	.00	.52	.21	.00	.00
3	0.002	1003	2015	2973	.01	.09	.30	-.02	.01	.18	.43	.00	.53	.18	-.01	.00
3	0.008	935	2086	3126	.01	.11	.34	.02	-.04	.31	.58	.04	.60	.27	.05	-.04
Actual	-	1000	2000	3000	.00	.10	.30	.00	.00	.20	.40	.00	.50	.20	.00	.00

The total time for all the identification runs listed in Table 1 was 10,000. The sampling interval was 100—a total of 100 samples each. The table shows that in most cases, the identification procedure was able to estimate all the flows and volumes to within $\pm 20\%$. As the amplitude of the noise increases, the system parameters are identified less accurately. If the noise is increased significantly beyond that shown ($\sigma^2 > 0.008$), the algorithm is unable to adequately identify any of the parameters and becomes unstable. For the case of no noise, the identification algorithm was able to predict the system parameters to within $\pm 10\%$ in all cases and usually much closer. For all of the simulations, the inputs were assumed to be impulses which mixed instantaneously with all of the air within the zone.

Figures 2 thru 7 show the 'real time' estimation of the parameters for the three-zone case. Figures 2 thru 4 indicate that when there is little noise in the data, the estimated parameters converge to steady-state values shortly after the impulses. Also, the parameters converge to their final, correct values, only after all of the zones have been pulsed. This is because all of the modes of the system are not suitably excited by the impulses unless they are applied to all of the zones.

Figures 5 thru 7 indicate that when there is significant noise ($\sigma^2 = 0.002$) associated with the data, the character of the least-squares solution changes considerably. The noise has the effect of slowing the convergence of the solution. Between the impulses, there is a considerable amount of random oscillation before the parameters settle down and approach steady values. Figure 7 indicates that the calculation of the effective volumes of the zones is much less sensitive to noise than that of the flows. The figure also indicates that the effective volume of each zone is determined immediately after the pulse and varies little thereafter.

All the figures show that the identified parameters steady-out sometime shortly after the previous pulse. Thus, when all of the parameters are changing only slightly with each new sample, then it is appropriate to apply an input to another zone. Also,

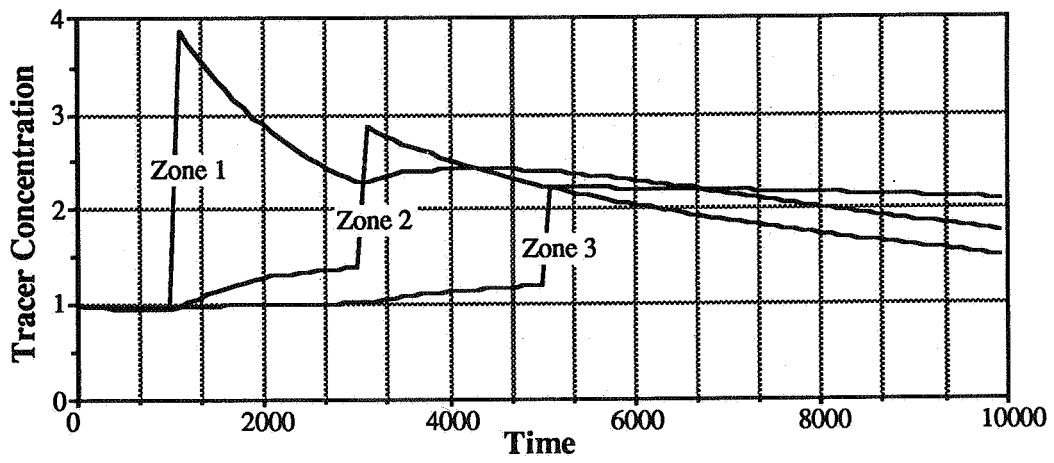


Figure 2. Tracer Concentrations for Three-Zone Simulation (No Noise)

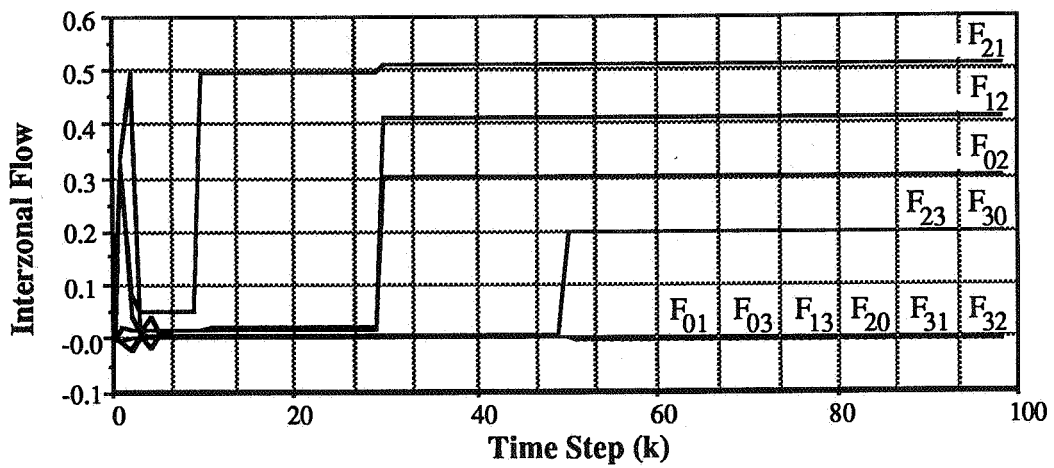


Figure 3. Interzonal Airflows Calculated using Recursive Least-Squares (No Noise)

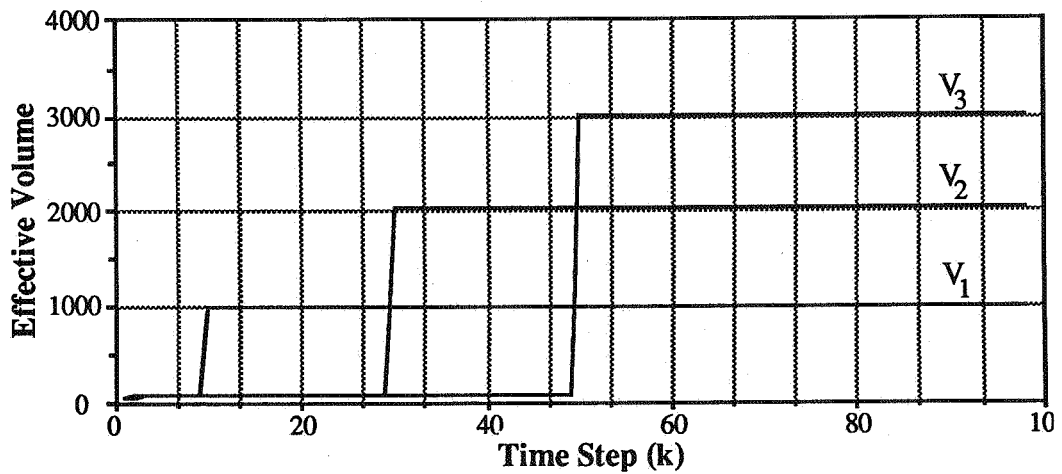


Figure 4. Effective Volumes Calculated using Recursive Least-Squares (No Noise)

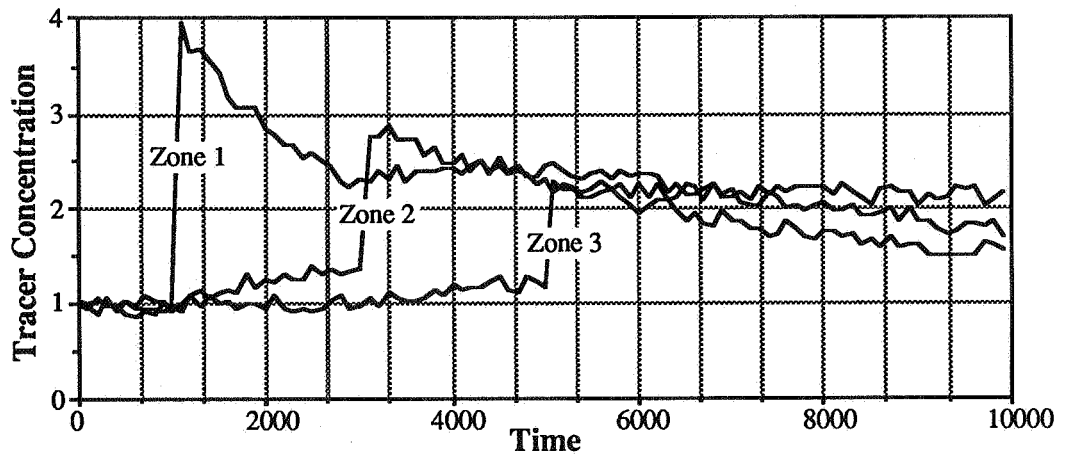


Figure 5. Tracer Concentrations for Three-Zone Simulation ($\sigma^2 = 0.002$)

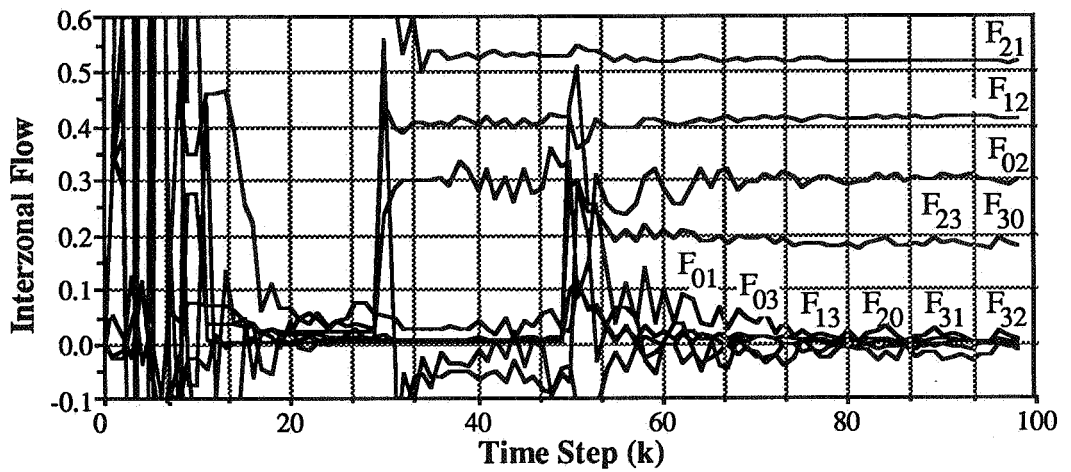


Figure 6. Interzonal Airflows Calculated using Recursive Least-Squares ($\sigma^2 = 0.002$)

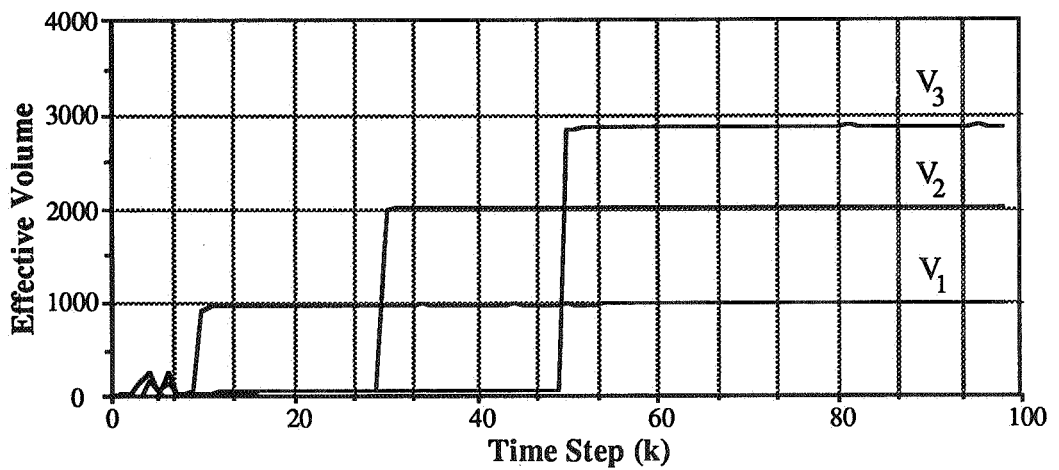


Figure 7. Effective Volumes Calculated using Recursive Least-Squares ($\sigma^2 = 0.002$)

as described above, a sampling interval of 100 was used in all of the identification runs listed in Table 1. This interval proved adequate for the cases shown. However, as the unmeasured disturbances to the system and the number of zones increases, the selection of the sampling interval becomes more important. Choosing a sampling interval which is either too small or too large can result in incorrect parameter estimation or instability of the identification algorithm

7. INPUT REQUIREMENTS FOR COMPLETE IDENTIFICATION

The identification of a dynamic system using the least-squares technique requires that the input which is applied to the system provide sufficient excitation. Another way of stating this is that the input must independently activate all of the modes of the system. In most control systems literature, an input which is often used to ensure that this condition is satisfied is a pseudorandom binary sequence (Jensen³) Unfortunately, to apply this type of input requires well regulated and calibrated equipment capable of providing real time readings of the flow rate of tracer into each zone at each sampling interval.

The identification runs described in the preceding section used inputs which were rapid injections (impulses). This type of input proved to be adequate for complete identification of the systems in question. It is also believed that an impulse type injection is practical to implement. A near impulse injection could be achieved by the rapid discharge of a pressurized cylinder or bursting a balloon filled with a known amount of tracer.

The simulations indicate that as each additional pulse is applied to the system, more parameters are identified. The simulations also reveal that all of the unknown flows and effective volumes are not determined until after an impulse has been applied to each zone. Thus, the conclusion can be drawn that for the impulse type input, sufficient excitation for complete system identifiability is achieved only by applying an impulse to all of the zones. Also, as will be discussed in the next section, if system parameters are varying, multiple impulses over time are required to track the parameters.

It was mentioned in the previous section that a new input should be applied as soon as possible after the preceding one. The natural question to ask is how close the inputs can be applied to one another and still result in satisfactory identification of the system parameters. To test this, the identification algorithm was run for the two-zone system examined in the previous section ($\sigma^2 = 0.002$). Two different input intervals were examined. In the first case, the impulse inputs were applied simultaneously (Figure 8). Both of the inputs were applied at $t = 2000$.

Figure 9 shows how the least-squares algorithm responded to the applied inputs. The figure indicates that the calculated flows take a considerable amount of time to approach their correct values—doing so only after an additional 100+ time steps following the applied inputs. Figure 8 also indicates that the tracer concentration in Zones one and two was considerably different after the two were pulsed with tracer. Further simulations have shown that as this difference is reduced, the identification algorithm becomes ill conditioned. It was also noticed that noise affects the identification procedure more significantly for the case of simultaneously applied inputs.

Figures 10 and 11 show the results of a nearly identical simulation. The only difference is that the inputs applied to the two zones are separated by 10 sample periods. Examination of Figure 11 indicates that the effect of this slight separation is to significantly improve the conditioning of the identification procedure. The inputs are applied to the zones at time steps 20 and 30. The figure also indicates that the identification is essentially complete by time step 40. This is a significant improvement over the simultaneous pulse results. Thus, while it appears possible to apply simultaneous inputs to each zone and still identify the parameters of interest,

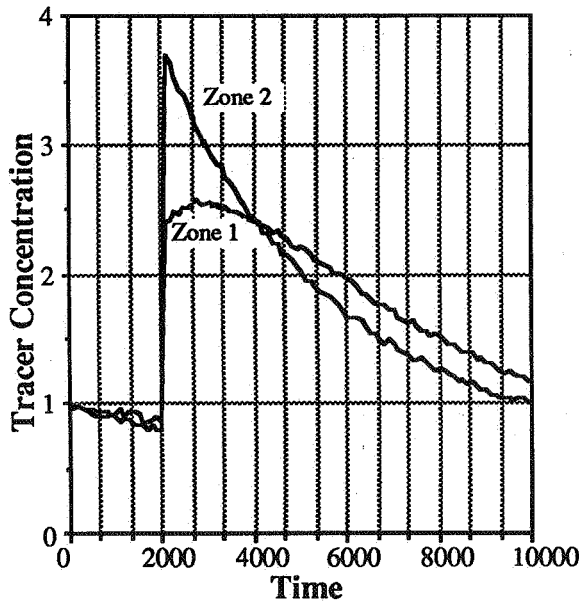


Figure 8. Data for Simultaneous Impulse Injection Input

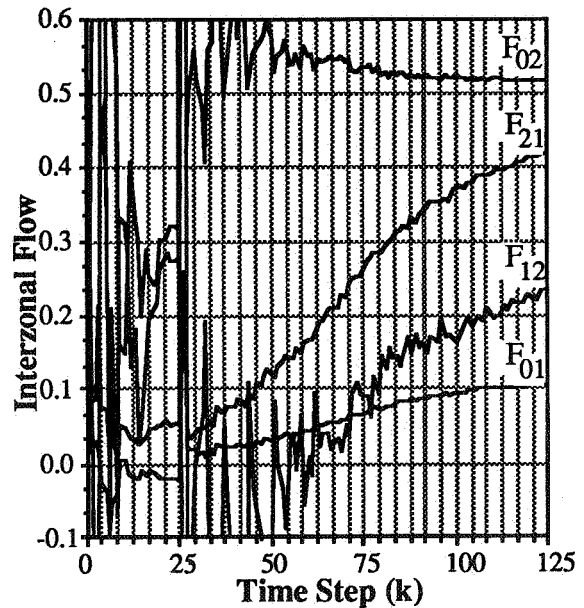


Figure 9. Calculated Flows for Simultaneous Impulse Injection Input

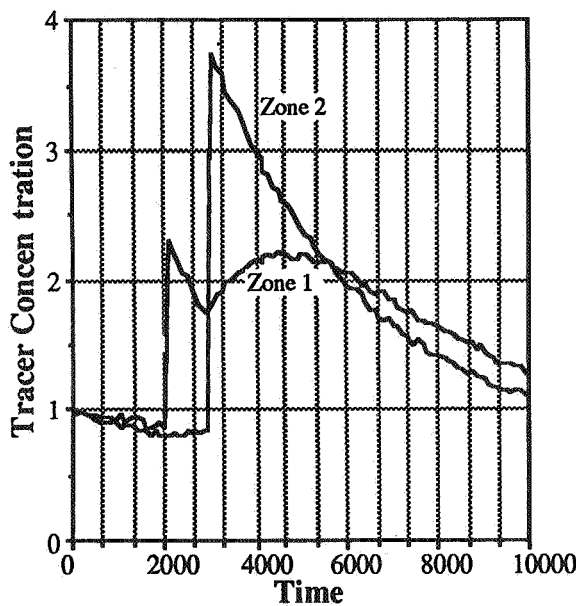


Figure 10. Data for Separated Impulse Injection Input

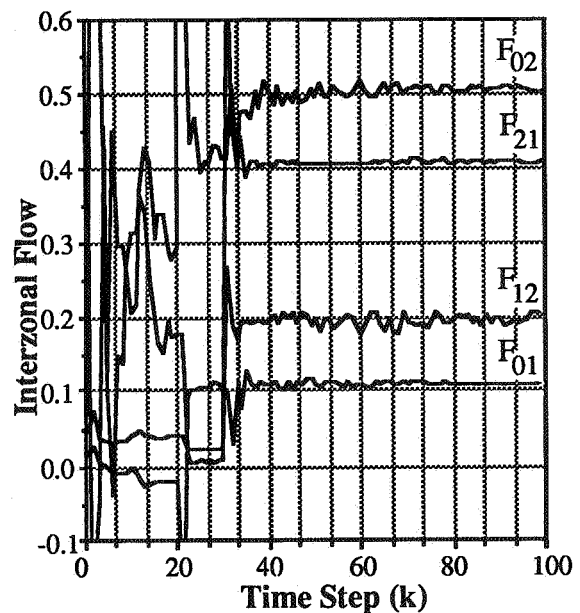


Figure 11. Calculated Flows for Separated Impulse Injection Input

the recursive least-squares algorithm is much more robust if the inputs are separated by several sample periods.

It should be noted that as the level of noise associated with the data is reduced toward zero (ie. the system becomes deterministic), the least-squares algorithm is able to identify the parameters much more rapidly. For simultaneous impulse inputs and clean data, the system is completely identified within 20 time steps following the inputs. However, even for clean data, separation of the inputs by a few time steps speeds the convergence of the least-squares algorithm.

8. VARYING FLOWS AND EFFECTIVE VOLUMES

The flows and effective volumes calculated using Equation (4.6) with $\beta(k) = 1$ are assumed to be constant for the duration of the test. If this assumption is not valid, the system parameters calculated by the least-squares analysis will be those which give the best overall fit of the data to the assumed system model and not necessarily the true values. If the system parameters are varying, then a slightly different approach must be followed when using the identification algorithm.

One of the primary purposes of obtaining the recursive formulation of the least-squares algorithm is for tracking the parameters in a system which is varying slowly with time. It should be noted that the approach presented below is not suited for identification of a system with high frequency parameter fluctuations. The variation in the parameters must be slow enough to allow the algorithm to 'catch' up with the new values before they change again significantly. If this condition is not satisfied, then the procedure will not work.

Equation (4.4) included the parameters, $\beta(k)$, and it was indicated that these parameters were a sequence which could give different weighting to the data during the recursive calculations. For example, proper selection of this sequence can reduce start-up transients which may pose problems if the data were very noisy. However, if $\beta(k)$ is assumed to have the form (Ljung¹⁰, Goodwin¹⁵)

$$\beta(k) = \lambda^{N-k} \quad (8.1)$$

where $0 < \lambda < 1$ then the algorithm is said to employ exponential forgetting of the data. The parameter, λ , is referred to as the forgetting factor. While in general, λ may also vary in time, in the following discussion, it is assumed a constant. The addition of this term effectively reduces the importance of data which were collected in the past and gives increasing weight to new data as they are recorded. Hence, if the flows and volumes are varying slowly, then this method can be used to track that variation in time.

This form of $\beta(k)$ also results in a slight modification of Equation (4.6). The recursive least-squares algorithm becomes

$$\hat{\theta}(k) = \hat{\theta}(k-1) + L(k)[y^T[k] - \phi^T(k-1)\hat{\theta}(k-1)] \quad (8.2a)$$

$$L(k) = \frac{P(k-1)\phi(k-1)}{\lambda + \phi^T(k-1)P(k-1)\phi(k-1)} \quad (8.2b)$$

$$P(k) = \frac{1}{\lambda} \left[P(k-1) - \frac{P(k-1)\phi(k-1)\phi^T(k-1)P(k-1)}{\lambda + \phi^T(k-1)P(k-1)\phi(k-1)} \right] \quad (8.2c)$$

Examination of Equation (8.2c) shows that the addition of exponential forgetting effectively keeps $P(k)$ from approaching zero, thus keeping the algorithm robust with respect to tracking.

The selection of the forgetting factor will have a substantial influence on the identification algorithm. Using a relatively small value of λ ($\lambda < 0.9$) will have the effect of discounting all but the last few data points. However, if substantial noise is associated with the data, the identification procedure will perform poorly and may become unstable. As λ approaches 1, the algorithm approaches that of the standard least-squares and all data are weighted equally. Thus, there exists a trade-off between noise considerations and the ability of the procedure to track varying parameters.

The use of the forgetting factor is shown in Figures 12 and 13 for the two-zone system described previously. Initially, the system is identical to that described in Table 1. However, at $t = 5000$, several of the system parameters associated with the second zone change: V_2 increases from 2000 to 3000, F_{02} drops from 0.5 to 0.3 and F_{20} decreases from 0.3 to 0.0. The data were noisy ($\sigma^2 = 0.002$) and a forgetting factor of 0.97 was used during the identification.

The inputs are applied to Zone 1 at $t = 1000$ and 6000 and applied to Zone 2 at $t = 2500$ and 7500 . Figure 12 shows that the algorithm is able to follow the flow parameters reasonably well with some fluctuation occurring around the times of the impulses. Figure 13 indicates that the algorithm is able to follow the effective volumes but only after the zone in which the volume changed is pulsed a second time.

In simulations using clean data, the algorithm was able to respond in a manner similar to that shown in Figure 3. The new values of the system parameters were all accurately identified (with little fluctuation) a few time steps after the conclusion of the second round of impulses. As might be expected, a more exciting input is required for identification of the time varying system parameters. If an impulse type input is being used as the excitation, it has been found that each zone must receive multiple inputs.

One final note on the selection of the value of the forgetting factor, λ . If the system is noisy, a value of λ less than 0.95 is usually not satisfactory for the cases studied. The algorithm becomes too sensitive to the random fluctuations induced by the unmeasured disturbances and does a poor job in tracking the system parameters. However, if very clean data are available, it is possible to use forgetting factors of 0.95 or slightly less.

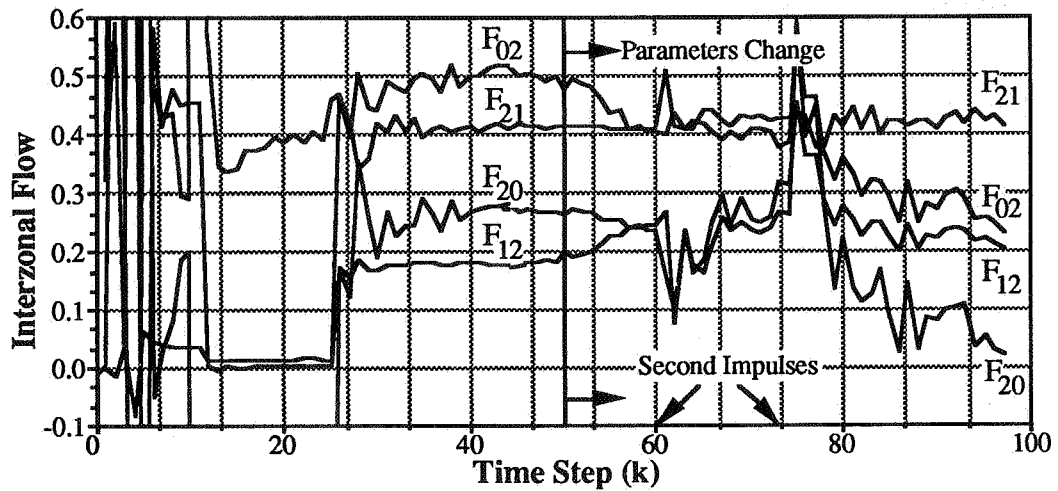


Figure 12. Interzonal Airflows Calculated using a Forgetting Factor ($\lambda = 0.97$)

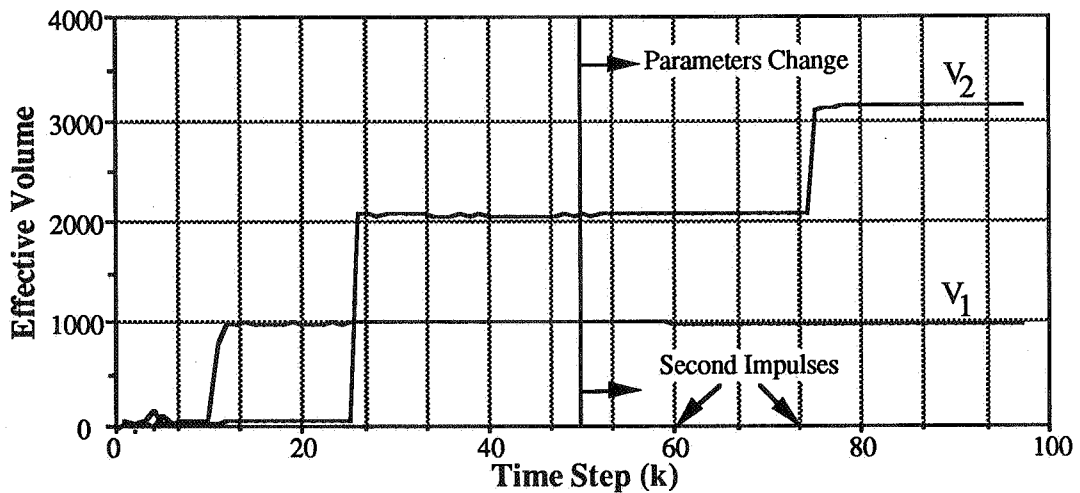


Figure 13. Effective Volumes Calculated using a Forgetting Factor ($\lambda = 0.97$)

9. SAMPLING INTERVAL

In the past several sections little mention was made as to how the sampling interval was chosen. However, selecting the correct sampling interval can make the difference between successful identification of the unknown system parameters or complete failure. Either the least-squares algorithm produces erroneous results or becomes unstable.

In choosing some 'optimal' (optimal in the sense that the system is accurately identified) sampling interval, there are two different though related considerations which must be addressed. First, the sampling interval must be rapid enough to capture the fastest dynamics of importance within the system. Sampling too slowly, with respect to the fastest system eigenvalue, will result in poor identification of the overall system. Second, the sampling interval must be slow enough to allow adequate mixing of the inputs between the injection and the first sample following it.

9.1 Sampling Interval and Eigenvalue Locations

The question of selecting an optimal sampling interval with respect to capturing important system dynamics has been studied by several researchers (Sinha¹⁶, Sinha¹⁷, Puthenpura¹⁸). A rule of thumb which is often mentioned by these authors is that the sampling interval should be chosen such that

$$|\mu T| \leq \Delta \quad (9.1)$$

where μ is the eigenvalue with the largest magnitude (fastest) in the continuous-time system. The value of Δ is usually in the range $0 < \Delta \leq 0.5$. In examining the criterion presented in Equation (9.1) two questions come to mind. First, since an unknown system is being identified and the fastest eigenvalue is not a priori information, how can an appropriate sampling period be chosen? Second, why not sample as fast as possible to ensure that the criterion will be satisfied? The answer to both of these questions can be found by examining the transformation of the system eigenvalues when mapped from continuous-time to discrete-time.

Since the flow systems under study must be stable, (no unmeasured tracer is injected) all of the eigenvalues are located on the left side of the $\text{Im } sT$ axis as shown in Figure (14). If it is further assumed that the sampling criterion of Equation (9.1) is satisfied, then the eigenvalues of the continuous-time system must lie within the shaded regions in the sT -plane. Recall from Equation (3.7) that in going from the continuous time system to its discrete equivalent, the system matrix becomes

$$A = \exp[(V^{-1}F)T] \quad (9.2)$$

If μ is an eigenvalue of $V^{-1}F$ then $\omega = \exp(\mu T)$ is an eigenvalue of A . The figure also indicates that the consequence of this mapping is that the region in the sT -plane containing the eigenvalues of $V^{-1}F$ are compressed into the lens shaped region in the z -plane when the system is discretized.

The z -plane figure reveals a problem which can arise if the sampling interval is chosen to be too small. As smaller values of T are chosen, the region in which all of the discrete-time eigenvalues are located becomes smaller and moves closer to the point $1 + j0$ ($j = \sqrt{-1}$). The eigenvalues found outside of the circle with radius $r = 1$ are unstable. If there is appreciable noise associated with the data then the identification algorithm may calculate values of the A matrix which have unstable eigenvalues. This will result in poor conditioning of the least-squares identification algorithm.

A number of identification runs were conducted to determine the best value of Δ for an impulse type input. Table 2 shows the results for the one, two, and three-zone systems described in Section 6. The table indicates that the sampling interval has a significant impact upon the accuracy of the identification algorithm. With no noise in the data, it is possible to use very small values of the sampling interval. This results in a very accurate estimate of the unknown flows and volumes. However, the accuracy appears to deteriorate as the sampling interval is raised past $\mu T \approx 0.1$.

As noise is added to the data ($\sigma^2 = 0.002$), the behavior of the least-squares algorithm changes. Table 2 shows that selection of a sampling interval which is too small decreases the accuracy of the identification procedure and can, in some cases, result in numerical instability. However, if the 'correct' sampling interval is chosen,

the accuracy of the identified parameters for the case of noisy data is similar to the corresponding case without noise.

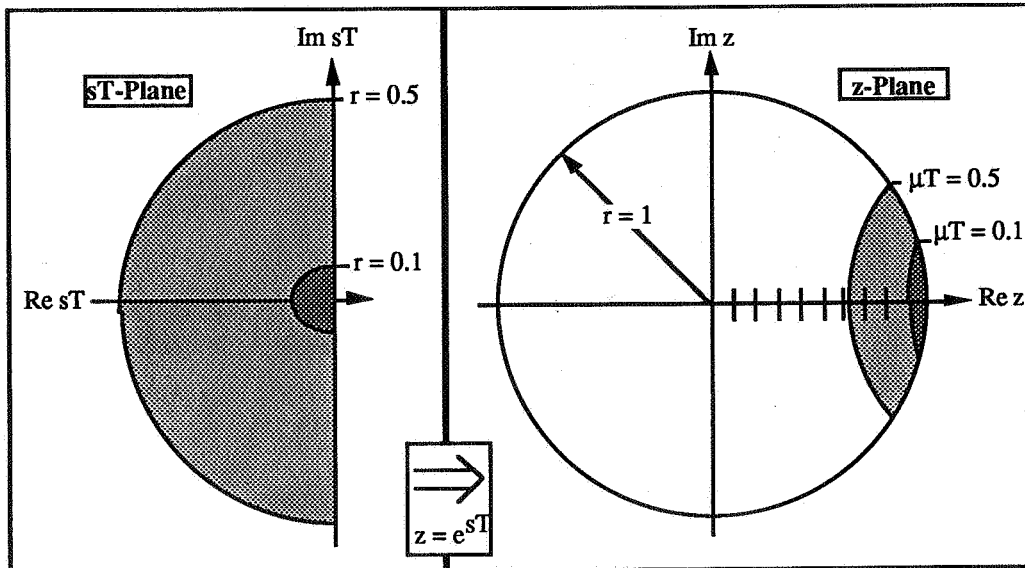


Figure 14. Eigenvalue Mapping using Criterion of Equation (9.1)

Table 2. Accuracy of Identification Algorithm with Different Sampling Intervals

# Zones	ω_{\max}	ω_{\min}	$ \mu_{\max} T $	Max. Error in Calculated Parameters(%) Without Noise	Max. Error in Calculated Parameters(%) With Noise
1	-	0.998	0.002	0.1	10
	-	0.940	0.06	5	5
	-	0.900	0.10	5	5
	-	0.821	0.20	11	12
	-	0.552	0.60	40	42
2	0.997	0.996	0.004	0.2	30
	0.979	0.938	0.06	10	24
	0.959	0.880	0.13	15	16
	0.900	0.731	0.30	51	50
	0.810	0.527	0.60	110	124
3	0.999	0.995	0.005	0.2	Unstable
	0.993	0.928	0.07	2.5	16
	0.991	0.900	0.10	4.0	9
	0.987	0.861	0.15	11	18
	0.967	0.687	0.40	22	211

Thus, proper selection of the sampling interval is critical for accurate identification of system parameters. A criterion for this selection can be established by examining the second, third, and fourth columns of Table 2. For very small values of the sampling interval, the eigenvalues of the discrete-time system are close to one another and to the point $1 + j0$. This is a point of potential instability in the algorithm. Fortunately, as the sampling interval is increased, the eigenvalues of the discrete-time system spread out and shift toward the left. As these eigenvalues change, the accuracy of the identified parameters improves up to the point where the smallest eigenvalue is in the range $0.88 < \omega < 0.92$. This corresponds to selection of the

value of μT such that $0.083 < |\mu T| < 0.13$. Therefore, for the simulations shown, a value of $\Delta \approx 0.1$ should be used when following the criterion for sampling interval selection described by Equation (9.1).

9.2 Sampling Interval and Effective Volumes

The effective volume that the analysis predicts for each zone also depends upon how well the impulse is dispersed between the time that it is injected into the zone and the first sampling of the concentration in that zone after the impulse (O'Neill⁷). In an attempt to better understand this relationship, it is useful to determine the conditions for which a two-zone system can be adequately represented as a single zone as shown in Figure 15. In the two-zone model shown on the left, if the interzonal flows (F') are sufficiently high relative to the external flows (F_0), then an impulse of tracer gas into either zone should be quickly dispersed throughout both zones and the concentrations in each should approach each other rapidly.

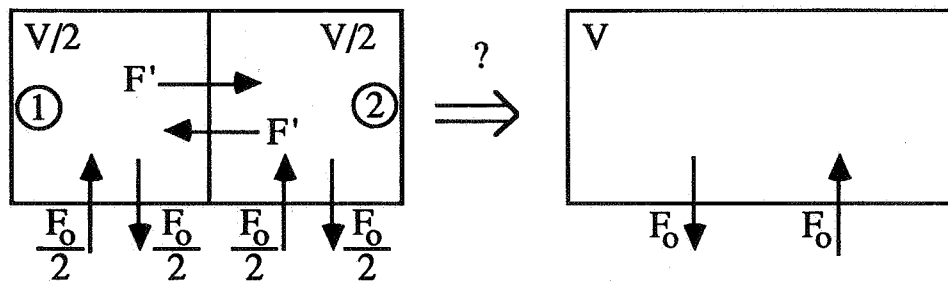


Figure 15. Two-Zone versus One-Zone Model for Least-Squares Analysis

The response of both zones to a single impulse of tracer gas (g_1) to Zone 1 can be determined by analytically solving Equation (3.3) for two zones to give an expression for the difference in zone concentrations (Δc) as a function of time, volume, and airflow rates as shown below.

$$\Delta c(t) = c_1(t) - c_2(t) = \left(\frac{2g_1}{V}\right) e^{-t(F_0 + 4F')/V} \quad (9.3a)$$

$$= \Delta c(0) e^{-t(1 + 4F'/F_0)/(V/F_0)} \quad (9.3b)$$

The term, $\Delta c(0)$, is the difference between the zone concentrations immediately after Zone 1 is pulsed. This equation shows that the concentration difference decays exponentially with time as the two zones mix. If the definitions, $\epsilon = \Delta c(t)/\Delta c(0)$ and $t^* = t/(V/F_0)$, are made, Equation (9.3) can be rewritten as

$$\frac{F'}{F_0} = -0.25 \left(\frac{\ln \epsilon}{t^*} - 1 \right) \quad (9.4)$$

The term, ϵ , indicates the difference in zone concentrations relative to the pulse disturbance and the term, t^* , is a nondimensional time based on the external air exchange rate of the zones. A criteria for uniform mixing can be defined by requiring that the concentration difference due to an impulse input (ϵ) must decay to certain value within a prescribed period of time (t^*). By specifying values for ϵ and t^* ,

Equation (9.4) can be used to determine the required relative interzonal airflow rate (F'/F_0) to assure uniform mixing. Figure 16 graphically relates the relationship given by Equation (9.4).

This figure indicates, for example, that a flow ratio of $F'/F_0 \approx 5$ is required to reduce ϵ to 0.1 within time $t^* = 0.1$. The simulation model was applied to a case where $V=1000$, $F_0=0.1$, and $F'=0.5$ ($F'/F_0=5$) with an impulse of tracer gas injected into Zone 1. Figure 17 shows how the concentration varies within the two zones as a function of $t^* = t/(10000)$ for a single impulse in Zone 1. The figure shows that, as expected, the difference in concentrations between the two zones decays to within 10% of the maximum value at $t^* \approx 0.1$.

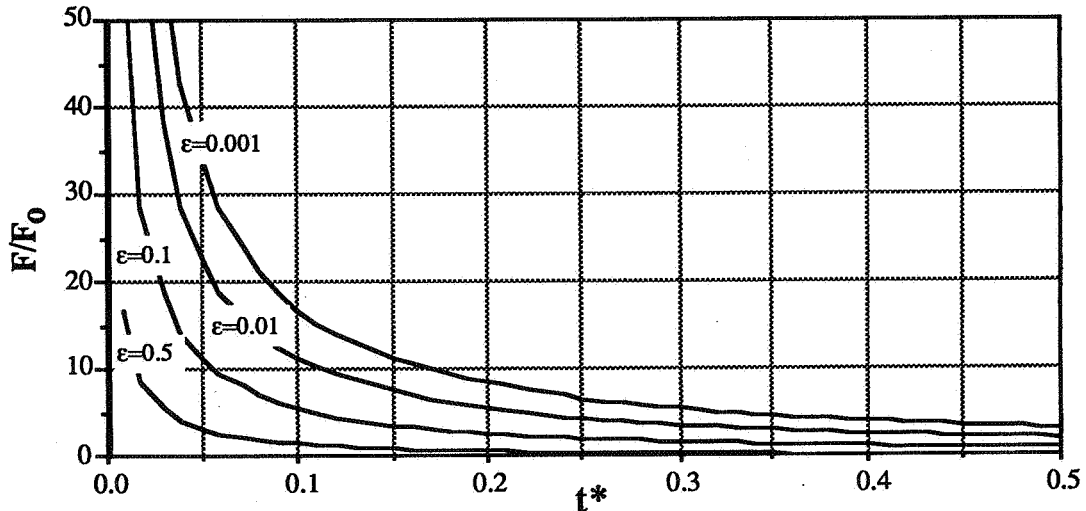


Figure 16. Ratio of F'/F_0 as a Function of t^* and ϵ

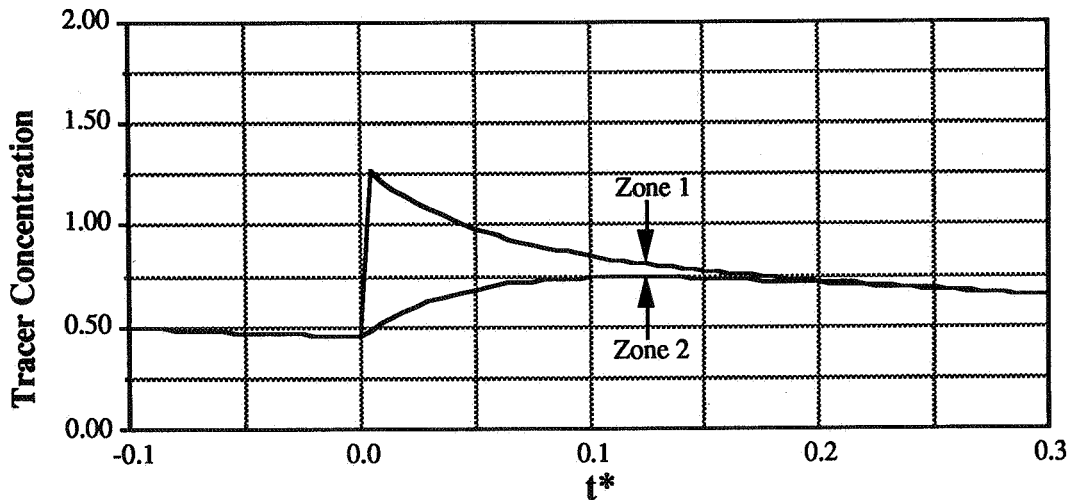


Figure 17. Tracer Concentration versus t^* For a Two-Zone System

The two-zone simulation model was used to generate data for several additional cases where Zone 1 is pulsed with a tracer gas and the recursive least-squares identification algorithm was used to determine the total effective volume, V , and external airflow rate, F_0 , for a corresponding single zone system based on the concentration data for Zone 1. The results are shown in Table 3 for various airflow rates and sampling intervals, $T^* = T/(V/F_0)$. For F'/F_0 less than 5, a single zone

approximation is unsatisfactory. However, as F/F_0 is increased to 5, a single zone approximation produces a flow and volume within 20% of the correct values of 0.1 and 1000 provided the appropriate sampling interval is chosen ($T^* = 0.1$). Numerous tests of the algorithm have indicated an approximate relationship between T^* , t^* , and ϵ . Using Equation (9.4), for a given F/F_0 , if one assumes $t^* \approx \epsilon$, the sampling period, T^* should be in the interval $0.1 < T^* \leq 0.2$.

Table 3. Single Zone Predictions for a Simulated Two-Zone System

2 Zone (Actual)				1 Zone (Predicted)		
F/F_0	V	F'	F_0	T^*	V	F_0
0.5	1000	0.05	0.10	0.005	501	0.08
1	1000	0.1	0.10	0.005	503	0.10
5	1000	0.5	0.10	0.005	521	0.15
5	1000	0.5	0.10	0.020	587	0.14
5	1000	0.5	0.10	0.100	901	0.12
10	1000	1.00	0.10	0.100	1023	0.11
115	1000	11.5	0.10	0.100	1004	0.10

Once it has been established that a single zone approximation of an actual two-zone system is possible under appropriate flow conditions, it is natural to wonder whether an extension to a three-zone system is possible. Here, the question considered is when can an actual three-zone system be modeled by a simplified two-zone approximation. In this case, the interzonal flows between zone 2 and 3 are varied relative to the outdoor flows (Figure 1). In the simulated three-zone system, $F_{02} = F_{03} = F_{20} = F_{30} = F_{21} = F_{31} = F_{12} = F_{13} = 0.5F_0$ ($F_0 = 0.1$), $F_{01} = F_{10} = 0.1$, $V_1 = 2V_2 = 2V_3 = 500$, and $F' = F_{23} = F_{32}$. The results of various simulations are summarized in Table 4. If the three-zone system is perfectly modeled as a two-zone system with Zones 2 and 3 behaving as a single zone (2), the following parameters would be predicted: $V_1 = V_2 = 500$ and $F_{12} = F_{21} = F_{01} = F_{10} = F_{02} = F_{20} = 0.10$. The table indicates that a two-zone approximation is valid provided the interzonal flows F_{23} and F_{32} are approximately ten times larger than F_0 . The simulations also indicate that the guidelines for sampling period described above have changed slightly. For the two-zone case, the sampling period should be based upon the characteristic time of the faster of the two zones. Then, using Equation (9.4), for a given F'/F_0 , if one assumes $t^* \approx \epsilon$, then the sampling period, T^* , should be in the interval $0.1 < T^* \leq 0.2$.

Table 4. Two-Zone Modeling of an Actual Three-Zone System

Three-Zone (Simulated)					Two-Zone (Predicted)						
V_1	$V_{2,3}$	F'	F_0	F'/F_0	T^*	V_1	V_2	F_{12}	F_{21}	F_{01}	F_{02}
500	250	0.01	0.01	1.0	0.020	504	255	0.007	0.009	0.012	0.008
500	250	0.05	0.01	5.0	0.020	504	271	0.009	0.016	0.011	0.011
500	250	0.05	0.01	5.0	0.100	525	371	0.010	0.014	0.011	0.011
500	250	0.05	0.01	5.0	0.400	632	610	0.015	0.015	0.011	0.011
500	250	0.10	0.01	10.0	0.020	504	293	0.009	0.018	0.010	0.012
500	250	0.10	0.01	10.0	0.100	531	458	0.011	0.012	0.010	0.011
500	250	0.10	0.01	10.0	0.200	565	539	0.012	0.012	0.011	0.011
500	250	1.00	0.01	100.0	0.004	501	336	0.010	0.021	0.010	0.018
500	250	1.00	0.01	100.0	0.010	502	443	0.010	0.012	0.010	0.011
500	250	1.00	0.01	100.0	0.020	505	495	0.010	0.010	0.010	0.010
500	250	1.00	0.01	100.0	0.040	510	512	0.011	0.011	0.010	0.011

At first glance, it may appear that we have developed two separate criteria for determination of sampling interval which may not be compatible. However, it turns out that satisfying the criterion established in Section 9.1 usually results in an acceptable 'mixing interval' for the input between the impulse and the first sample following it. For example, the continuous-time eigenvalue of interest for the two-zone system (with high interzonal airflows) described in Table 3 is $\mu = -(F_0/V) = -0.0001$. Satisfying the criterion established in Equation (9.1) requires that the sampling interval be $T = 1000$ ($|\mu T| = 0.1$). This results in a value of $T^* = 0.1$. For the purpose of system identification, Section 9.2 indicates that these two zones will be adequately described by a single zone if the concentration ratio between them is reduced to 0.1 within $t^* = 0.1$ ($t = 1000$).

10. IDENTIFYING THE NUMBER OF INTERCONNECTED ZONES

Before a successful tracer gas experiment can be undertaken, one of the most important parameters which must be determined is the total number of zones. Often, the physical characteristics of a building aid in this process. For example, individual rooms separated by doorways or corridors are often obvious choices for separate zones. However, there are other situations in which determining the number of zones is not as easy. For example, deciding whether a very large room is best modeled as one, two, or even three zones is often not a simple matter. Another difficulty might be in determining whether to combine a series of small well connected rooms into a fewer number of larger zones.

Thus, a method for determining the number of zones in a system would be useful to the analyst conducting tracer gas studies. Such information would be of particular interest in determining whether to break a larger zone up into smaller zones or combine a series of smaller zones into fewer larger ones. This would greatly increase the accuracy of the identification process which is, the goal of most tracer gas studies.

Consider again the system of discrete-time difference equations represented by Equation (3.6)

$$c(k+1) = A c(k) + B g(k) \quad (10.1)$$

If an output equation is defined as

$$y(k) = D c(k) \quad (10.2)$$

then the system of equations can be transformed from the state-space system of equations to an input-output formulation (Kuo⁹). Taking the z-transforms of Equations (10.1) and (10.2) and combining them produces

$$y[z] = D (zI-A)^{-1} B g(z) = W(z) g(z) \quad (10.3)$$

assuming D , A , and B are constant. The matrix $W(z)$ is known as the transfer function matrix and is the complex frequency matrix which 'filters' the inputs as they travel through the system. If D is assumed to be the identity matrix—that is, each output, $y_i(k)$ is simply equal to the concentration of tracer in that zone at time step k ,

then Equation (10.3) can be inverted back into the discrete-time domain. This results in the formation of n discrete-time input-output equations

$$y_i(k) = \sum_{j=1}^n p_{ij}y_i(k-j) + \sum_{j=1}^n a_{ij}g_i(k-j) + \sum_{h=1}^n \sum_{q=2}^n (1-\delta_{ih})b_{hq}g_h(k-q) \quad \{i = 1 \dots n\} \quad (10.4)$$

If a single input is applied to the zones, the double summation drops out and Equation (10.4) takes the form of the well known auto-regressive moving-average system (ARMA). ARMA systems appear often in control system theory and signal processing. A great deal of study has gone into methods for determining the order of an ARMA process by simply observing the input-output sequence (Akaike¹⁹, Bhansali²⁰, Soderstrom²¹, and Chen²²). Many of these methods rely upon a statistical test of the residuals of the least-squares fit of the parameters to the data.

A method known as the AIC criterion (Information Criterion-A), first introduced by Akaike¹⁹, has been found to produce consistent estimates of the order of multizone airflow systems using a single impulse input into one of the zones as the excitation. Let S[n] be the sum of the squared error between the actual output and the output predicted by an ARMA model of order n

$$S[n] = \sum_{k=1}^{N_{data}} (y_{i,act}(k) - y_{i,pred}^n(k))^2 \quad (10.5)$$

The AIC criterion for selection of model order is based upon maximizing the following function

$$AIC = 2 \ln\{L(S[n])\} - 2p \quad \{n = 1 \dots \text{max. order}\} \quad (10.6)$$

where p is the number of parameters associated with the chosen model order (p=2n). The term L(S[n]) is the maximum likelihood function. For the case where the noise superimposed upon the data is white the first term in Equation (10.6) is given by

$$2 \ln\{L(S[n])\} = -\frac{N}{2} (1 + \ln 2\pi + \ln\{S[n]/N\}) \quad (10.7)$$

Thus, the appropriate order of the system is given by the n which maximizes the AIC function.

Before describing the results of a number of computer simulations to verify the performance of the AIC criterion, it is necessary to describe the fundamental concepts of controllability and observability of a system from a prescribed input-output pair. In simplified terms, a multizone system which is completely controllable from an input $g_i(k)$ is one in which the concentration of tracer in any zone can be raised or lowered to any prescribed level by a judicious choice of $g_i(k)$ within a finite time interval. In a similar manner, a multizone system which is completely observable from an output $y_i(k)$ is one in which a change in tracer concentration in any of the zones will have some effect upon the value of the output, $y_i(k)$. Figure 18 illustrates the concepts of controllability and observability for a simple two-zone system. A number of tests exist for determining controllability and observability of a system from an input-output pair. However, these tests require a priori knowledge of the A matrix which is not available in the identification procedure.

The results of simulations conducted to test the AIC criterion are shown in Table 5. Simulations of actual one, two, and three-zone systems were run. In each case, the input was applied to Zone 1 a few time steps into the simulation and the output was the tracer concentration of Zone 1. and The data were then fit to Equation (10.4) for models up to fourth order and the resulting sums of the squared error were computed for each. Equation (10.6) was then used to calculate the AIC. For the two-zone case, the flows were varied to determine the effect that interzonal flows have upon the predicted model order. The results shown indicate that decreasing the flows between the two zones relative to the total flow reduces the likelihood of correctly predicting the order of the system.

For the three-zone case, the effective volumes of the zones were varied. Table 5 indicates that if all interzonal flows are equal, the effective volumes of all three zones must be substantially different before the AIC criterion is able to discern the presence of three different zones. It should also be noted that changing some or all of the interzonal airflows and/or initial tracer concentrations can have a similar effect.

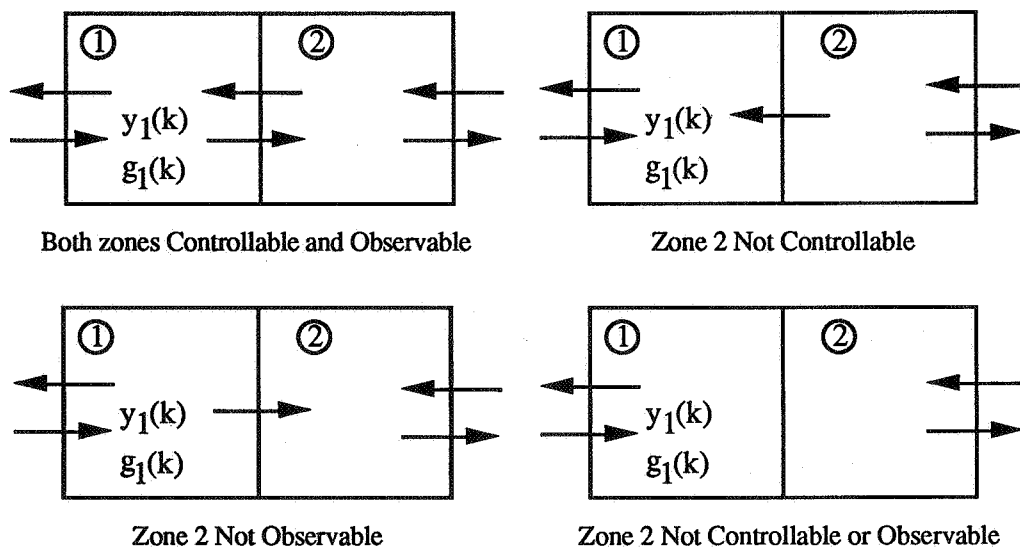


Figure 18. Examples Showing Conditions Under Which a Two-Zone is Controllable and Observable from Input-Output Pair $[g_1(k) y_1(k)]$

Table 5. Determination of Model Order Using AIC Criterion

Actual Number of Zones	Effective Volumes of Zones 1/2/3	Interzonal Airflows (all = 0.1 unless otherwise noted)	AIC Criterion			
			Number of Zones			
			1	2	3	4
1	1000	0.1	158	150	138	128
2	1000/1000	0.1	106	132	130	120
2	1000/1000	$F_{12}=F_{21}=0.5$	88	118	114	104
2	1000/1000	$F_{12}=F_{21}=0.02$	155	148	138	129
3	1000/1000/1000	0.1	78	132	131	120
3	1000/500/250	0.1	75	132	132	121
3	1000/500/100	0.1	67	129	131	120

Table 5 shows that under certain conditions, the AIC criterion will result in a correct prediction of the number of zones, n , in a multizone flow system. However, this number should be interpreted as only the minimum possible number of zones

which are required to adequately model the system. There may be more zones within the system which the procedure was not able to identify. There are two possible reasons for this. First, some of the zones may not be controllable or observable (or only weakly controllable and observable) from the input-output pair selected. In such a case, the dynamics of the system will not be completely captured using that choice of input-output pair. Second, as the number of actual zones is increased past 2, symmetries within the system make it difficult to separate the effect that different zones have upon the output. Thus, the more asymmetric a system is, with respect to effective volumes and interzonal flows, the more likely that the AIC criterion will identify a larger number of zones. If it is suspected that more zones may exist, it may be advisable to change locations of the input (impulse) and/or output (sensor), and repeat the test.

The AIC criterion is also sensitive to the sampling rate. As the sampling interval is decreased, the number of data points increases. This results in a larger sum of the squared error. When the number of data points becomes large, even with low noise, increasing the order of the model has only a slight effect upon the sum of the squared error and the AIC criterion predicts a lower number of zones. In the case of an extremely small sampling interval, increasing the model order will have little or no effect upon the sum of the squared error.

Conversely, using only a small number of data points (a large sampling interval) in conjunction with the AIC criterion will also produce erroneous results. In this case, increasing the order of the system will have a disproportionate effect upon the sum of the squared error. The AIC criterion will predict a larger number of zones than exist in the actual system. In the extreme case where the number of data points equals the number of model parameters, the sum of the squared error will be zero and the AIC criterion blows up.

Simulations have shown that the AIC criterion performs most accurately when a sampling interval of $T \approx 0.1\tau$ is used. The time constant, $\tau = (t_2 - t_1)$, is the time it takes for the zone tracer concentration to decay from the initial concentration following the impulse input, $c(t_1)$, to a concentration $c(t_2) = c(t_1)e^{-1}$. The total test time, t_{tot} should be approximately 2τ .

Once again, a guideline has been established for selection of the proper sampling interval. While this criterion may seem new, it is closely related to that established in Section 9.1 where the discrete-time eigenvalues were used to select an appropriate sampling interval. Unfortunately, when the system is transformed to an input-output representation, the eigenvalues become less accessible. In this case, it becomes necessary to look at the actual tracer decay curve to obtain an indication of the system eigenvalues and thus, obtain the sampling interval.

11. CONCLUSIONS

The recursive least-squares identification algorithm presented in this paper provides a method for accurate prediction all of the interzonal airflow rates and effective volumes of a multizone system. The algorithm requires that an input of tracer gas be applied to each zone of interest and uses the concentration data for each to calculate the unknown system parameters. In addition, this method shows potential for tracking flows and effective volumes in time varying systems.

The sampling period has also been shown to greatly affect the accuracy of the results. Careful selection of the sampling period is important both to the stability of the identification algorithm and to ensure proper mixing of the inputs between samples.

A method has also been introduced for determining the order of the system to be identified. This method, which uses the residuals of least-squares parameter fits of various model orders, can accurately predict the true system order under the appropriate conditions.

Work is underway on the construction of an experimental facility to verify some of these results. It should be noted that the conclusions and results reported above are limited to the specific cases examined in this paper and are not necessarily general. More work is needed to prove their applicability to more general cases and make refinements as necessary.

12. REFERENCES

1. Harrje, D. T. et. al. "Documenting Air Movements and Infiltration in Multicell Buildings Using Various Tracer-Gas Techniques". ASHRAE Technical Data Bulletin, Vol. 1, No. 2, 1985.
2. Afonso, C.F.A., Maldonado, E.A.B., Skaret, E.A. "Single Tracer-gas Method to Characterize Multi-room Air Exchanges". Energy and Buildings, 9, p. 273-80, 1986.
3. Jensen, L. "Determination of Flows and Volumes in Multiple Cell Systems". Proceedings of RoomVent-87, June 1988, Stockholm Sweden.
4. Axley, J., Persily, A. "Integral Mass Balances and Pulse Injection Tracer Techniques". U.S. Department of Commerce, NISTIR 88-3855, October, 1988.
5. Charlesworth, P. S. "Air Exchange Rate and Airtightness Measurement Techniques- An Applications Guide". AIVC Document AIC-AG-2-88, 1988.
6. Carolyn Allen. AIRGLOSS: Air Infiltration Glossary . AIC Technical Note 5, December, 1981.
7. O'Neill, P.J. and R. R. Crawford. "Development of an Interzonal Airflow Measurement Technique Using a Pulsed Tracer Gas". Transactions of Clima 2000. Sarajevo, Yugoslavia. August 27-September 1, 1989.
8. Sinden, F. W. Multi-Chamber Theory of Air Infiltration. Building and Environment, Vol. 13, 1978.
9. Kuo, B. C. Digital Control Systems. Holt, Rinehart, and Winston, Inc., New York, 1980.
10. Ljung, L., Soderstrom, T. Theory and Practice of Recursive Identification. The MIT Press, Cambridge, 1983
11. Eykhoff, P. Ed. Trends and Progress in System Identification. Pergamon Press, New York, 1981.
12. Kudva, P., Narendra, K. S. "An Identification Procedure for Discrete Multivariable Systems". IEEE Transactions on Automatic Control, pp. 549-52, October, 1974.
13. Ossman, K. A., Kamen, E. W., "Adaptive Regulation of MIMO Linear Discrete -Time Systems Without Requiring a Persistent Excitation". IEEE Transactions on Automatic Control, Vol. AC-32, No. 5, May 1987

14. Sinha, N. K., Lastman, G. J. "Identification of Continuous-Time Multivariable Systems from Sampled Data". *International Journal of Control*, Vol. 35, No. 1, pp. 117-126, 1982
15. Goodwin, G. C., Sin, K. S. Adaptive Filtering Prediction and Control. Prentice-Hall, Inc., New Jersey, 1984
16. Sinha, N. K., Lastman, G. J., Zhou, Q. J., "On the Choice of the Sampling Interval for the Identification of Continuous-Time Systems from Sampled Data". *Proceedings of the 25th Midwest Symposium on Circuits and Systems (Houghton, MI)* pp. 328-32 1982.
17. Sinha, N. K., Kuszta, B. Modeling and Identification of Dynamic Systems. Van Nostrand Reinhold Company, New York, 1983.
18. Puthenpura, S., Sinha, N. K. "A Procedure for Determining the Optimal Sampling Interval for System Identification Using a Digital Computer". *Canadian Electrical Engineering Journal*, Vol. 10, No. 4, pp. 152-7, 1985
19. Akaike, H., "A New Look at the Statistical Model Identification". *IEEE Transactions on Automatic Control*, Vol. AC-19, No. 6, pp. 716-23, 1974.
20. Bhansali, R. J., Downham, D. Y. "Some Properties of the Order of an Autoregressive Model Selected by a Generalization of Akaike's EPF Criterion". *Biometrika*, Vol. 64, No. 3, pp. 547-51, 1977.
21. Soderstrom, T. "On Model Structure Testing in System Identification". *International Journal of Control*, Vol. 26, No. 1, pp. 1-18 , 1977.
22. Chen, H-F., Guo, L. "Consistent Estimation of the Order of Stochastic Control Systems". *IEEE Transactions on Automatic Control*, Vol. AC-32, No. 6, June 1987.

Discussion

Paper 7

Mike Holmes (Ove Arup, London UK)

Can the method be used to look at the general mixing in a single zone? For example the distribution of pollutants?

Patrick O'Neil, Roy R. Crawford (University of Illinois, USA)

Yes, we believe that a zone's response to the impulse type input is closely related to the internal mixing characteristics of that zone. An integral part of our ongoing research effort is to analyze systems in which it takes a significant amount of time for the inputs to mix within the zone(s). By simply analyzing the impulse response of a zone, we hope to be able to characterize, in some sense, the mixing characteristics of that zone.

Bjorn Hedin (Lund Institute of Technology, Sweden)

There are some advantages of using the PRBS input: by theory, the discrete time description (3.6) requires that the input is constant during the sample period. The PRBS fulfils this demand, but a short impulse injection doesn't, i.e. such impulses will violate the sampling theorem. This can lead to extra estimation errors. The PRBS input will neither violate the assumption of ideal mixing as obviously as the short impulse. Do you want to comment on these things?

Patrick O'Neil, Roy R. Crawford (University of Illinois, USA)

Certainly. As you mentioned, the impulse type input, as described in this paper, may not satisfy the criterion of constant inputs between sample periods. However, the simulations which we have run indicate that this should not be a significant problem. If necessary, you could assume that the impulse was evenly distributed over a single sample interval. In addition to the fact that an impulse input is easier to apply to a zone, we also believe that it gives you additional information on the mixing characteristics of the zone.

Bjorn Hedin (Lund Institute of Technology, Sweden)

Why do you use the recursive least-square (LS) method? You don't have use of the advantage which is a short execution time, but suffer from the disadvantage of higher sensitivity to noise (or even breakdown at higher noise levels). The common or batch LS method can never be unstable, it's fast enough, and it's easy to use "forgetting factors" in this method as well.

Patrick O'Neil, Roy R. Crawford (University of Illinois, USA)

If the recursive method causes difficulty during the data analysis, then one can certainly fall back upon the batch method which I have described. However, depending upon the computing power available, there may be utility in using the recursive method when analyzing very "fast" systems.

Bjorn Hedin (Lund Institute of Technology, Sweden)

The volume matrix V is calculated as $V = B^{-1}R$ (eg. 5.6, page 9).

But the chance to receive a diagonal volume matrix from multiplication of two filled matrices doesn't seem to be very big, especially not when the estimations of B and R are disturbed by noise. How do you interpret the non-zero off-diagonal elements in $V = B^{-1}R$? Can they be ignored?

Patrick O'Neil, Roy R. Crawford (University of Illinois, USA)

In most of the simulations, the off-diagonal elements have been 1 or 2 orders of magnitude smaller than the diagonal elements. Consequently, these elements were ignored. However, if noise and/or mixing problems result in volume matrices with significant off-diagonal elements, then using methods which constrain them may become necessary.

Max Sherman (LBL, California, USA)

The linear least squares technique used - which is a standard control theory approach - has some severe limitations as presented. You have linearized the exponential solution which requires a short time step in the analysis, however, at a small time step the concentration is highly autocorrelated and cannot be simply regressed. You must take into account the (non-diagonal) covariance matrix. Since this is a physical system (cf a control system), a chi-squared analysis system with the real covariance matrix is a more appropriate approach.

Patrick O'Neil, Roy R. Crawford (University of Illinois, USA)

Our next step is to validate the proposed method using a three-zone experimental facility which we are developing. We will look at these types of issues as they arise.

Max Sherman (LBL, California, USA)

The multizone, single gas technique you propose is biased unless one has a constant flow rate over the analysis. Thus it is not well suited for time vary systems unless you use a series of pulses and analyze different sets of pulses separately. The relaxation model you propose is not appropriate for this kind of system.

Patrick O'Neil, Roy R. Crawford (University of Illinois, USA)

No indirect method (as all tracer techniques are) for analyzing flows within buildings is well suited for tracking rapidly varying flows. However, if the flows are varying slowly, we believe this method is as appropriate as any.

Max Sherman (LBL, California, USA)

When using real data (as opposed to simulated) you will find that the noise in the concentration is far from "white". One's analysis technique must be quite robust to handle this. Furthermore, all of the parameters are intrinsically and experimentally correlated. It is, therefore, quite important to do a complete error analysis. I look forward to seeing this next year with measured data.

Patrick O'Neil, Roy R. Crawford (University of Illinois, USA)

Again, as we collect experimental data, we will look more closely at these issues.